J Nanostruct Chem (2014) 4:117
DOI 10.1007/s40097-014-0117-y

ORIGINAL

Visual sensing of Hg^{2+} using unmodified Au@Ag core–shell nanoparticles

Lihua Li · Dexiang Feng · Xian Fang · Xiaowei Han · Yuzhong Zhang

Received: 19 May 2014 / Accepted: 19 June 2014 / Published online: 24 July 2014

Abstract In this work, we have developed a novel visual Hg^{2+} sensor in aqueous solution using unmodified Au@Ag core–shell nanoparticles at room temperature, based on a redox reaction between Ag-shell and Hg^{2+}. The prepared Au@Ag core–shell nanoparticles exhibited good monodispersity. In the presence of Hg^{2+}, Hg^{2+} was reduced into Hg (0) by Ag-shell, and deposited on the surface of Au-core to form Au–Hg alloys and caused nanoparticles aggregation, leading to the color changes of the solution from yellow to purplish red, and the surface plasmon resonance spectra of Au@Ag core–shell nanoparticles red shift. Under the optimal conditions, the visual sensor could selectively detect Hg^{2+} as low as 0.4 μM with the naked eye and 5.0 nM by UV–vis spectra analysis methods. The designed sensor had several advantages: (1) the nanoparticles surface need not be functionalized. (2) The color change of the solution was in 2 s and could easily be observed with naked eyes. The visual sensor had been applied to detection of Hg^{2+} in tap and lake water, which obtained satisfied result.

Keywords Visual sensor · Hg^{2+} · Au@Ag core–shell nanoparticles

L. Li · D. Feng · X. Fang · X. Han · Y. Zhang (✉)
Anhui Key Laboratory of Chemo-Biosensing, College of Chemistry and Materials Science, Anhui Normal University, Wuhu 241000, People's Republic of China
e-mail: zhyz65@mail.ahnu.edu.cn

L. Li · D. Feng
Department of Pharmacy, Wannan Medical College, Wuhu 241002, People's Republic of China

Introduction

Monitoring of toxic heavy metal ions has received much attention because these metal ions are extremely hazardous and can exert adverse effects on the environment and on human health. Mercury ion (Hg^{2+}), which is widely distributed in the air, water, and soil, is considered to be one of the most toxic and dangerous metal pollutants because it can damage the brain, nervous system and the immune system [1–4]. Therefore, various methods have been developed for Hg^{2+} detection including electrochemical methods [5, 6], optical detections [7–9], immunoassay sensors [10, 11].

However, many methods previously need expensive instruments, complex treatment process and cost longer time. So, it is important to develop a simple and sensitive method for the Hg^{2+} detection.

Recently, visual detection based on Au nanoparticles (Au NPs) and Ag nanoparticles (Ag NPs) is attractive due to the color changes which are easily observed with naked eyes and no sophisticated instruments [12–16]. For example, Chai et al. [17] reported a visual detection of Hg^{2+} using L-cysteine functionalized gold nanoparticles. Laxman et al. [18] presented a visual method for selective recognition of Hg^{2+} based on inducing the aggregation of CPB-capped Ag NPs. However, these methods need to functionalize the surface of Au NPs or Ag NPs such as DNA [19], aptamer [20], thio compounds [21], fluorescent dyes [22] or polymers [23], etc. It is apparent that the functionalized procedures are tedious and readily contaminated.

To overcome these drawbacks, in recent years, bimetallic core–shell nanoparticles, which are a combination of two kinds of metal elements, have obtained a considerable attention in the detection of heavy metal ions. For instance, Xin et al. [24] reported a colorimetric detected trace Cr(VI)

ion based on the redox etching of Ag@Au nanoparticles at room temperature. Lou et al. [25] reported a visual detection of Cu^{2+} based on catalytic leaching of Au@Ag nanoparticles. Although the surface of these core–shell nanoparticles need not be functionalized, the detection process needs longer time and the sensitivity of methods was not high.

As is well known, the redox reaction can occur between Ag (0) and Hg^{2+} (the standard potential of Ag^{+}/Ag and Hg^{2+}/Hg is 0.80 and 0.85 V, respectively).When the Hg^{2+} is reduced, the reduced Hg (0) can deposit on the surface of Au NPs to form Hg–Au alloys due to Au which has a strong affinity for mercury. Inspired by the knowledge above, we designed a novel strategy for Hg^{2+} determination based on a redox reaction between Ag-shell of Au@Ag core–shell nanoparticles (hereinafter Au@Ag NPs)and Hg^{2+}. In the absence of Hg^{2+}, Au@Ag NPs exhibit good spherical monodispersity, and in the presence of Hg^{2+}, the reduced Hg (0) would deposit on the surface of Au-core to form Hg–Au alloys. The formation of Au–Hg alloys caused the nanoparticles aggregation, leading to the color changes of the solution from yellow to purplish red. Therefore, the color change can be used to visual sensing of Hg^{2+}. The method obtained is simple and could be used to the detection of Hg^{2+} in tap and lake water.

Experimental

Materials

Chloroauric acid ($HAuCl_4{\cdot}4H_2O$), silver nitrate ($AgNO_3$) and trisodium citrate dehydrate ($C_6H_5Na_3O_7{\cdot}2H_2O$) were purchased from Sinopharm Chemical Reagent Co. Ltd. (Shanghai, China). L-ascorbic acid was from Aladdin Reagents Co, Ltd. (Shanghai, China). All other chemicals used in this work were analytical reagent grade. All solutions were prepared with twice-quartz-distilled water. The water sample was from Jinghu Lake (Wuhu, China) and tap water was from our laboratory.

Instruments

The absorption spectra were obtained on a U-3010 UV–vis-NIR spectrometer (Hitachi, Japan). The morphology and the size of the Au NPs and Au@Ag NPs were measured by a scanning electron microscope (SEM) using JE0LJSM-6700F microscope (Hitachi, Japan).

Preparation of Au NPs

Au NPs were prepared according to previously described process [26]. In brief, a 50.0 mL of 0.01 % $HAuCl_4$ was heated to boiling. Next, 2.0 mL of 1 % trisodium citrate was added under stirring vigorously, and kept boiling until the solution became wine red. Finally, the solution was cooled to room temperature while stirring. The diameter of the Au NPs was measured about 16 nm by SEM.

Preparation of Au@Ag NPs

Au@Ag NPs were prepared according to previously described method with a little modification [27]. Simply, as-prepared Au NPs (1.0, 1.5, 2.0, 2.5 and 3.0 mL) were added to each of five 50 mL round-bottomed flasks containing 10 mL of water, respectively. Next, 0.1 mL of 38.8 mM trisodium citrate and 0.1 mL of 10 mM ascorbic acid were added dropwise to the above solution under stirring. Finally, 0.25 mL of 10 mM $AgNO_3$ was added dropwise each flask while stirring. The resulting solutions were stirred for 30 min until the colors of the solutions changed from pink to yellow. The products obtained were collected for further used.

Visual detection of Hg^{2+}

For visual detection of Hg^{2+}, the pH of the system (2.0 mL of Au@Ag NPs) was adjusted to 4.5 with the citric acid–sodium hydrogen phosphate buffer saline. Then, different concentrations of Hg^{2+} were added separately to the above solution; the color changes could be observed with naked eye; and the absorption curves were recorded at room temperature.

Analysis of real samples

To invest the practical application capability of this sensor, all the collected samples were centrifuged for 15 min at 9,000 rpm, and the supernatant was filtered through a 0.2 μm membrane. Then, a series of samples were prepared by spiking standard solutions of Hg^{2+} to the lake water or tap water. The pretreated samples were added to 2.0 mL of Au@Ag NPs (pH 4.5) and then were analyzed using the developed sensing strategy.

Results and discussion

Investigation of sensing mechanism

The sensing mechanism of Hg^{2+} using Au@Ag NPs is probably related to a redox reaction between Ag-shell and Hg^{2+} [the standard potential of 0.8 V (Ag^{+}/Ag) and 0.85 V (Hg^{2+}/Hg), respectively]. In the absence of Hg^{2+}, the prepared Au@Ag NPs exhibited good spherical monodispersity (the monodispersity is related to excessive

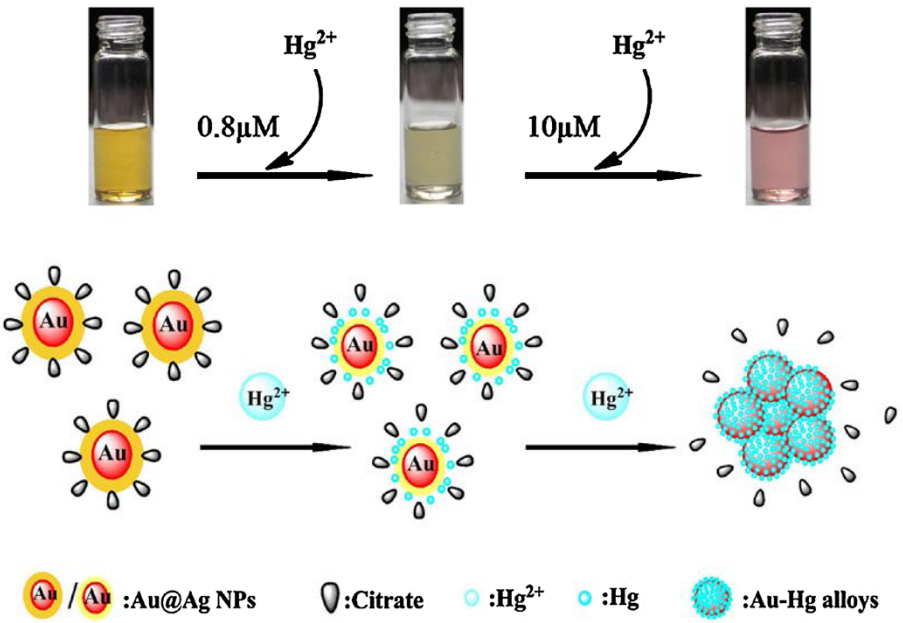

Scheme 1 Possible mechanism and schematic illustration for the visual sensing of Hg^{2+} using unmodified Au@Ag NPs

citrate ions in the solution) (seen in Fig. 1c). In the presence of Hg^{2+}, a redox reaction between Ag-shell and Hg^{2+} would occur. The Ag-shell became thinner and the sizes of Au@Ag NPs decreased gradually due to the oxidation of Ag-shell. The color of the solution changed lighter (from yellow to faint yellow), the surface plasmon resonance (SPR) absorption peak blue-shifted gradually, and the intensity decreased. When the concentration of Hg^{2+} was up to 10 μM, the color of the solution changed from yellow to purple red, and the SPR absorption peak red-shifted due to the strong affinity between Hg and Au NPs, the reduced Hg (0) would directly deposit onto the surface of Au-core to form Au–Hg alloys (Scheme 1). During these processes, citrate ions were kept off the surfaces of nanoparticles, leading to aggregation of nanoparticles (seen in Figs. 1d, 4a).

It was reported that citrate ions on the surface of Au NPs could also reduce Hg^{2+} to form Au–Hg alloys and caused aggregation [28]. To make it clear whether the redox reaction was from Hg^{2+} and Ag-shell or Hg^{2+} and citrate ions in our system, we design a contrast experiment to investigate the reaction mechanism. Namely, 20 μL of Hg^{2+} (1 mM) was added to 2.0 mL solution of citrate-stabilized Au NPs and citrate-stabilized Ag NPs, respectively (the concentration of Hg^{2+} was 10 μM). It was observed that the color of Au NPs solution changed nothing, the intensity and position in the SPR absorption peaks of Au NPs also did not change in the absence and presence of the Hg^{2+}. On the contrary, in the presence of Hg^{2+}, the solution color of Ag NPs changed from yellow to colorless, and the SPR absorption peaks of Ag NPs disappear. In addition, Energy-dispersive X-ray (EDX) analysis showed the elementary Ag in the agglomerates was basically no left while the content of Hg was higher (seen in Fig. 1e). These facts showed that the formation of Au–Hg alloys was from the redox reaction between Ag-shell and Hg^{2+} rather than between citrate ions and Hg^{2+}.

The absorption spectra of Au@Ag NPs

When different amounts of Au seeds (1.0–3.0 mL) were added to the solution, the absorption spectra of Au@Ag NPs were located at 404, 398, 394, 392 and 389 nm, respectively (seen in Fig. 1a).It could be observed that the intensity of SPR absorption decreased gradually as the concentration of Au seeds increased, accompanying with the blue shifts and broadening of absorption peak. The solution color of the prepared Au@Ag NPs changed from light yellow to deep yellow. The phenomenon could be explained that the optical properties of Au@Ag NPs were dominated by Ag at low concentration of Au seeds, and it was dominated by Au as the concentration of Au seeds increased.

Optimization of the experiment conditions

To optimize the experiment conditions, 20 μL Hg^{2+} (1 mM) was injected into the five kinds of the different ratios of Au/Ag Au@Ag NPs solutions (2.0 mL), respectively. The solution color changed from yellow to purplish red, and a new absorption peak which appeared at about 520 nm accompanying with the original SPR absorption peaks disappeared. The intensity of the new absorption peak was increased as the concentration of Au seeds increased (Seen in Fig. 1b). We observed that the color

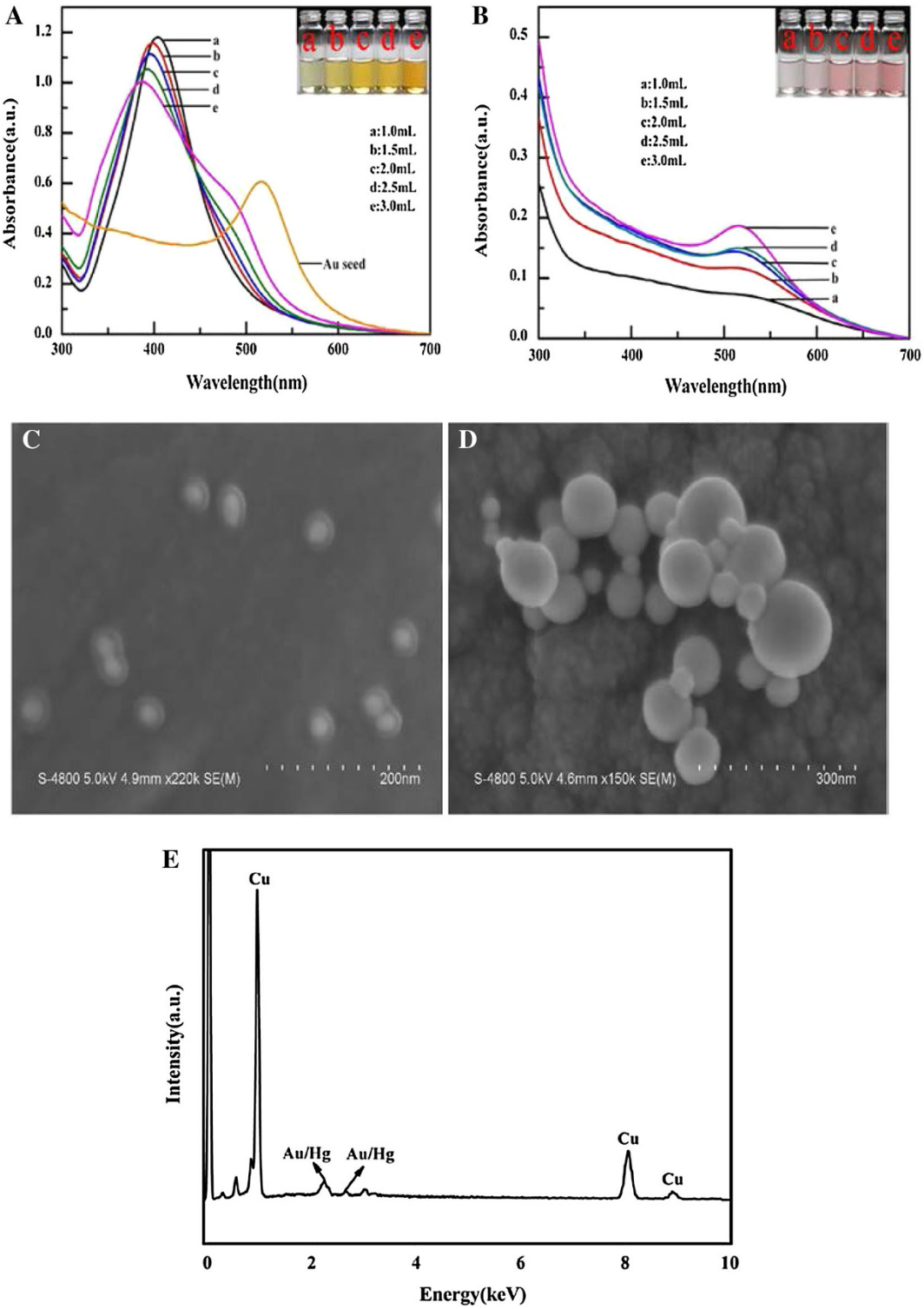

Fig. 1 UV–vis absorbance spectra and the photographic images of the prepared Au@Ag NPs with different Au seed volumes in the absence (**a**) and the presence (**b**) of 10 μM Hg^{2+}, respectively. SEM images of Au@Ag NPs with 1:3 molar ratio of Au/Ag (namely 2 mL Au seed) in the absence (**c**) and the presence (**d**) of 10 μM Hg^{2+}, respectively. (**e**) EDX spectra of Au@Ag NPs with 1:3 molar ratio of Au/Ag in the presence of 10 μM Hg^{2+}

changes of Au@Ag NPs solution with 1.0, 1.5 mL Au seeds were not easy to be observed by naked eyes; in addition, we also observed that the two kinds of nanoparticles solution were difficult to centrifuge before and after addition of Hg^{2+}, so Au@Ag NPs obtained from the 1.0, 1.5 mL Au seeds need not be adopted in this work.

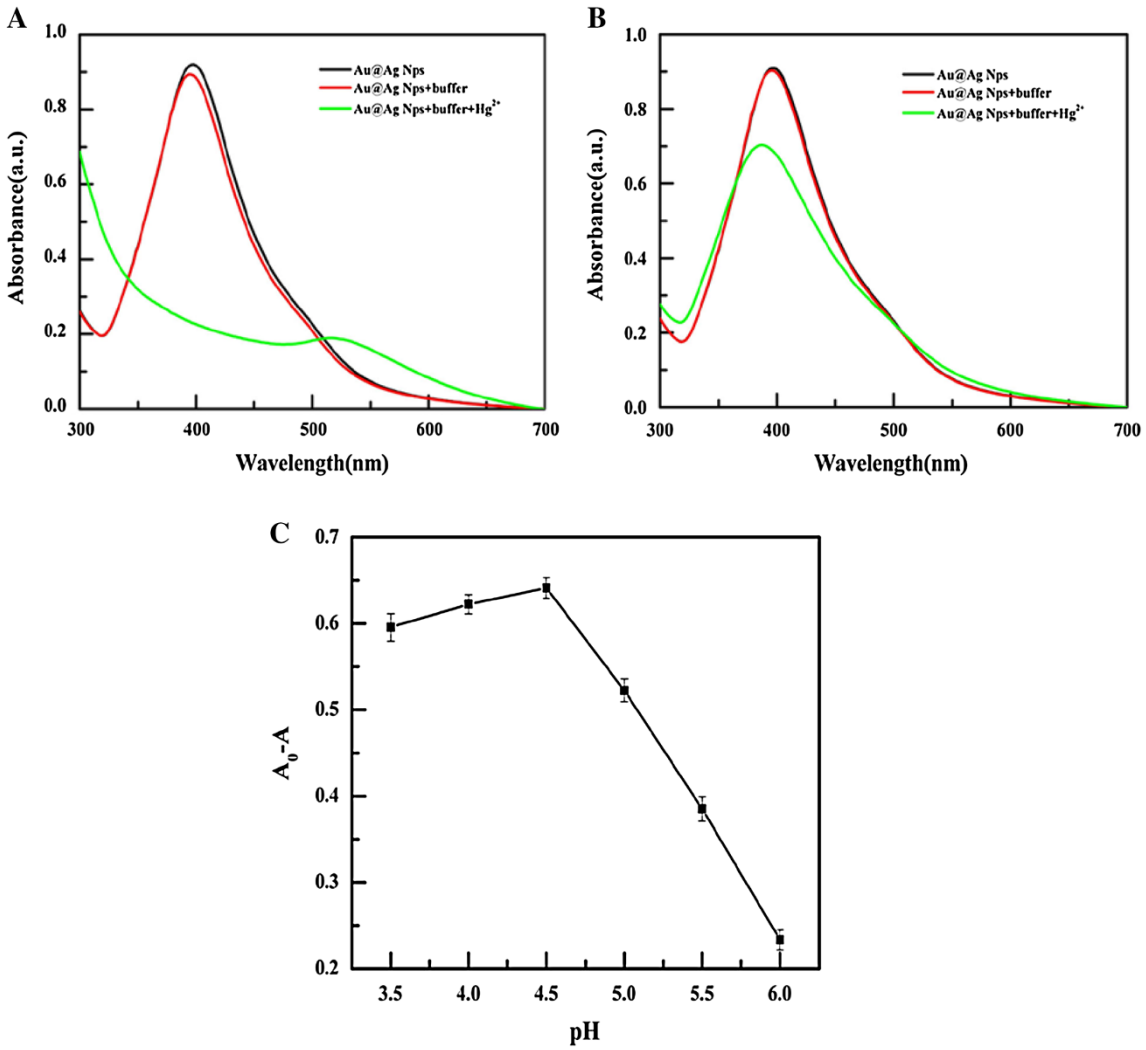

Fig. 2 The effect of pH on the of Hg^{2+} detection. UV–vis absorbance spectrum of Au@Ag NPs in the presence of pH 3.5 (**a**), pH 6.0 (**b**) and the (A_0–A) value of Au@Ag NPs (at 394 nm) containing the 10 μM Hg^{2+} under different pH conditions (3.5–6.0) (**c**)

From the view of peak shape, the color changes and the maneuverability, 2.0 mL Au seeds were chosen in this work. The SEM images of the Au@Ag NPs showed a good spherical monodispersity and the diameter was about 40 nm. EDX spectra showed that the molar ratios of Au/Ag were 1:3.

The effect of pH was also investigated in the absence and presence of Hg^{2+}. The pH of the system was adjusted in the range of 3.5–6.0 using the citric acid–sodium hydrogen phosphate buffer saline (pH 2.2–7.0) and the results obtained are shown in Fig. 2. It was observed that the stability of Au@Ag NPs was related to the pH of the system. Simply, if pH was lower than 3.5, the stability of Au@Ag NPs would decrease (seen in Fig. 2a). As pH increases, the stability of Au@Ag NPs was improved; however, if the pH was higher than 6.0, the color of the solution did not change in the presence of Hg^{2+}, and the decline of the SPR absorption intensity was not clear (seen in Fig. 2b). From Fig. 2c, it could be observed that Au@Ag NPs were stable and the changes of the SPR absorption spectra were obvious in presence of pH 4.5. Hence, a pH of 4.5 was employed in this study.

Selectivity

To investigate selectivity of sensor, some foreign metal ions including Li^{+}, Na^{+}, K^{+}, Mg^{2+}, Ca^{2+}, Ba^{2+}, Zn^{2+}, Mn^{2+} Co^{2+}, Fe^{2+},Cu^{2+},Cd^{2+} Cr^{3+}, Ni^{2+}, Hg^{2+} were selected for this study. Figure 3a shows the photographs of solutions in the presence of various foreign metal ions. It was clearly observed that the existence of about 50-fold of Li^{+}, Na^{+}, K^{+}, Mg^{2+}, Ca^{2+}, Ba^{2+}, Mn^{2+}, Zn^{2+}, Fe^{2+}, Ni^{2+}, and tenfold of Co^{2+}, Cu^{2+}, Pb^{2+} and the same concentration of Cd^{2+} and Cr^{3+} did not interfere the

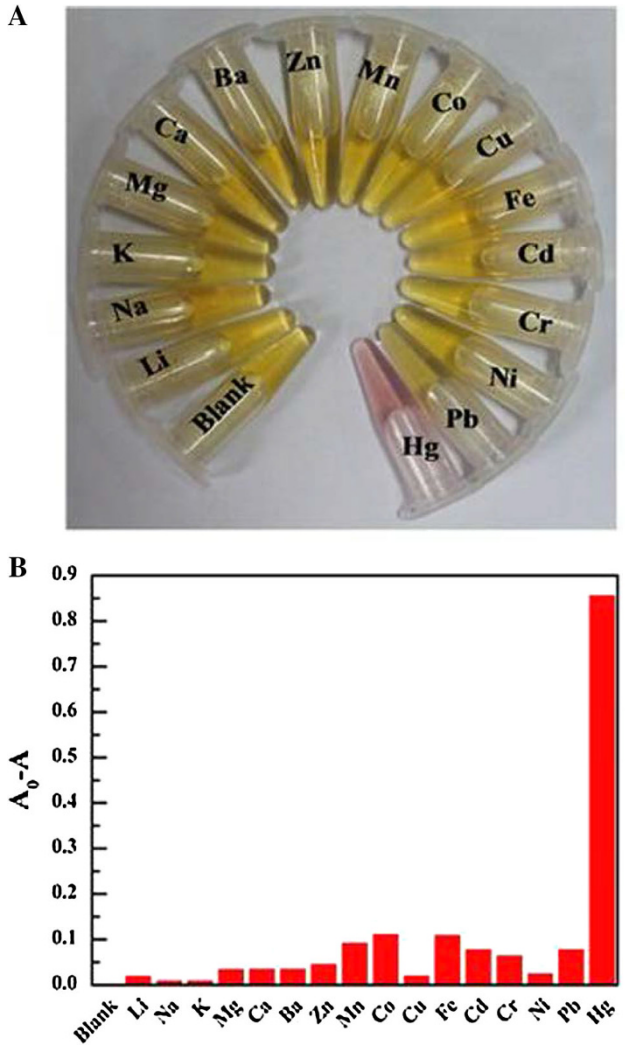

Fig. 3 Photographs (**a**) and the (A_0–A) values (**b**) (at 394 nm) of 2 mL Au@Ag NPs solution upon addition of various metal ions, respectively, at pH 4.5. Concentration: 10 μM Hg^{2+}; 500 μM Li^+, Na^+, K^+, Mg^{2+}, Ca^{2+}, Ba^{2+}, Mn^{2+}, Zn^{2+}, Fe^{2+} and Ni^{2+}; 100 μM Co^{2+}, Cu^{2+} and Pb^{2+}; 10 μM Cd^{2+} and Cr^{3+}

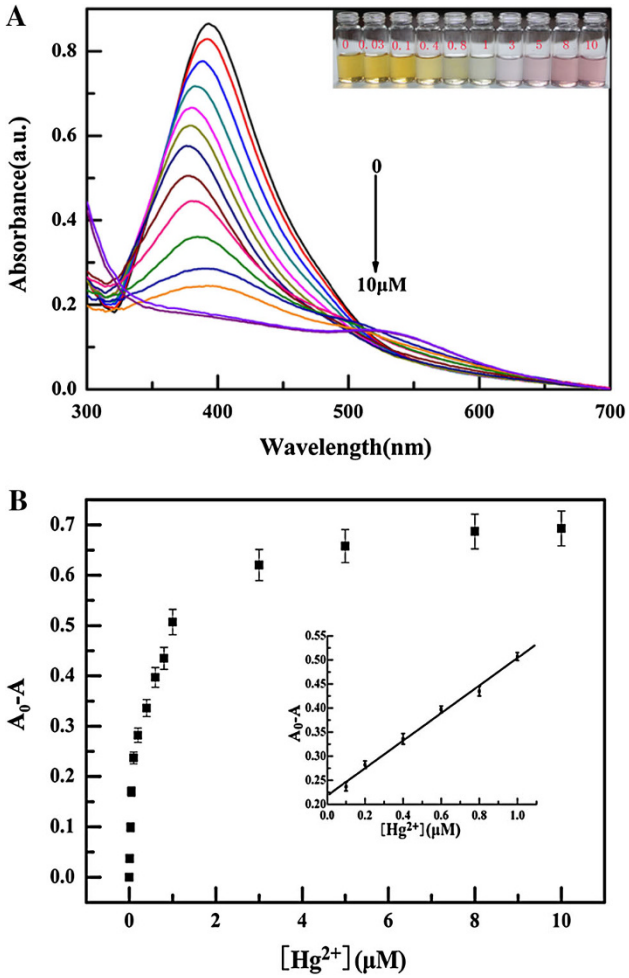

Fig. 4 **a** UV–vis absorbance spectrum of 2.0 mL Au@Ag NPs solution in the presence of Hg^{2+} concentration (0–10 μM) at pH 4.5. Inset: the photographs of 2.0 mL Au@Ag NPs solution in various Hg^{2+} concentration. **b** Plot of (A_0–A) values versus Hg^{2+} concentration, $\lambda = 394$ nm. Inset: a linearity of Hg^{2+} at a concentration range from 0.1 to 1 μM

determination of Hg^{2+}. Hg^{2+} was only the ion, which resulted in distinct color change from yellow to purplish red, indicating that this sensor has good selectivity.

Analytic performance

To investigate the sensitivity of the sensor, the Au@Ag NPs were utilized for sensing Hg^{2+} under the optimized conditions, and the results are shown in Fig. 4. As the concentration of Hg^{2+} increased from 0 to 10 μM, the color of the Au@Ag NPs gradually changed from yellow to purplish red. In the meantime, the intensity of the absorption peak at 394 nm decreased gradually. Specially, when the concentration of Hg^{2+} was up to 8 μM, a new absorption peak appeared at about 520 nm, indicating the formation of Au–Hg alloys. The decline of the intensity was linear with the concentration of Hg^{2+} increased in the range of 0.1–1.0 μM. The linear regression equation was $\Delta A = 0.2178 + 0.2862c$ (Here, $\Delta A = A_0 - A$. A_0 and A stand for the absorbance of solution in the absence and presence of Hg^{2+}, respectively; the unit of concentration is μM) with the correlation coefficient of 0.996. The limit of detection was about 0.4 μM with the naked eye and 5.0 nM by UV–vis measurements.

Analysis of real samples

To test the application of the proposed approach, we selected lake water and tap water samples for Hg^{2+} detection. The results are shown in Table 1, the recovery of Hg^{2+} was within 82.4–112.0 % for tap water and 83.6–115.0 %

Table 1 The result of Hg^{2+} determination in real samples ($n = 3$)

Samples	Added (μM)	Found (μM)	Recovery (%)	RSD (%)
Tap water	ND			
	0.100	0.824	82.4	0.67
	0.200	0.191	95.5	1.26
	0.400	0.448	112.0	1.58
	0.600	0.588	98.0	0.83
Lake water	ND			
	0.100	0.836	83.6	1.22
	0.200	0.230	115.0	0.72
	0.400	0.434	108.5	0.95
	0.600	0.610	101.7	1.61

ND not detected

for lake water, respectively, indicating that the sensor was suitable for the detection of Hg^{2+} in real samples.

Conclusions

In summary, a visual sensor has been developed for the sensitive and selective detection of Hg^{2+} using unmodified Au@Ag NPs. The changes of solution color and the peak intensities were readily obtained in the Hg^{2+} detection. The merits of the visual sensing lie in its simplicity, speed and convenience.

Acknowledgments This work was financially supported by the National Natural Science Foundation of China (Grant No. 20675002).

References

1. Lavoie, R.A., Jardine, T.D., Chumchal, M.M., Kidd, K.A., Campbell, L.M.: Biomagnification of mercury in aquatic food webs: a worldwide meta-analysis. Environ. Sci. Technol. **47**, 13385–13394 (2013)
2. Holmes, P., James, K.A.F., Levy, L.S.: Is low-level environmental mercury exposure of concern to human health? Sci. Total Environ. **408**, 171–182 (2009)
3. Clarkson, T.W., Magos, L., Myers, G.J.: The toxicology of mercury-current exposures and clinical manifestations. N. Engl. J. Med. **349**, 1731–1737 (2003)
4. Wang, Y., Yang, F., Yang, X.: Colorimetric biosensing of mercury (II) ion using unmodified gold nanoparticle probes and thrombin-binding aptamer. Biosens. Bioelectron. **25**, 1994–1998 (2010)
5. Zhang, Z., Tang, A., Liao, S., Chen, P., Wu, Z., Shen, G., Yu, R.: Oligonucleotide probes applied for sensitive enzyme-amplified electrochemical assay of mercury (II) ions. Biosens. Bioelectron. **26**, 3320–3324 (2011)
6. Lai, Y., Ma, Y., Sun, L., Jia, J., Weng, J., Hu, N., Yang, W., Zhang, Q.: A highly selective electrochemical biosensor for Hg^{2+} using hemin as a redox indicator. Electrochim. Acta **56**, 3153–3158 (2011)
7. Guha, S., Roy, S., Banerjee, A.: Fluorescent Au@Ag core–shell nanoparticles with controlled shell thickness and Hg II sensing. Langmuir **27**, 13198–13205 (2011)
8. Cheng, X.H., Li, Q.Q., Li, C.G., Qin, J.G., Li, Z.: Azobenzene-based colorimetric chemosensors for rapid naked-eye detection of mercury(II). Chem. Eur. J. **17**, 7276–7281 (2011)
9. Li, C.Y., Zhang, X.B., Qiao, L., Zhao, Y., He, C.M., Huan, S.Y., Lu, L.M., Jian, L.X., Shen, G.L., Yu, R.Q.: Naphthalimide-porphyrin hybrid based ratiometric bioimaging probe for Hg^{2+}: well-resolved emission spectra and unique specificity. Anal. Chem. **81**, 9993–10001 (2009)
10. Date, Y., Aota, A., Terakado, S., Sasaki, K., Matsumoto, N., Watanabe, Y., Matsue, T., Ohmura, N.: Trace-level mercury ion (Hg^{2+}) analysis in aqueous sample based on solid-phase extraction followed by microfluidic immunoassay. Anal. Chem. **85**, 434–440 (2013)
11. He, H., Wu, F., Xu, M., Yang, S.G., Sun, C., Yang, H.: Development and validation of a competitive indirect enzyme-linked immunosorbent assay for the determination of mercury in aqueous solution. Anal. Methods **3**, 1859–1864 (2011)
12. Ding, N., Zhao, H., Peng, W.B., He, Y.J., Zhou, Y., Yuan, L.F., Zhang, Y.X.: A simple colorimetric sensor based on antiaggregation of gold nanoparticles for Hg^{2+} detection. Coll. Surf. A. **395**, 161–167 (2011)
13. Chansuvarn, W., Imyim, A.: Visual and colorimetric detection of mercury (II) ion using gold nanoparticles stabilized with a dithia–diaza ligand. Microchim. Acta. **176**, 57–64 (2012)
14. Fan, Y.J., Liu, Z., Wang, L., Zhan, J.H.: Synthesis of starch-stabilized Ag nanoparticles and Hg^{2+} recognition in aqueous media. Nanoscale Res. Lett. **4**, 1230–1235 (2009)
15. Farhadi, K., Forough, M., Molaei, R., Hajizadeh, S., Rafipour, A.: Highly selective Hg^{2+} colorimetric sensor using green synthesized and unmodified silver nanoparticles. Sens. Actuat. B. **161**, 880–885 (2012)
16. Wang, G.L., Zhu, X.Y., Jiao, H.J., Dong, Y.M., Li, Z.J.: Ultrasensitive and dual functional colorimetric sensors for mercury (II) ions and hydrogen peroxide based on catalytic reduction property of silver nanoparticles. Biosens. Bioelectron. **3**, 337–342 (2011)
17. Chai, F., Wang, C.G., Wang, T.T., Ma, Z.F., Su, Z.M.: L-cysteine functionalized gold nanoparticles for the colorimetric detection of Hg^{2+} induced by ultraviolet light. Nanotechnology **21**, 025501–025506 (2010)
18. Walekar, L.S., Gore, A.H., Anbhule, P.V., Sudarsan, V., Patila, S.R., Kolekar, G.B.: A novel colorimetric probe for highly selective recognition of Hg^{2+} ions in aqueous media based on inducing the aggregation of CPB-capped AgNPs: accelerating direct detection for environmental analysis. Anal. Methods **5**, 5501–5507 (2013)
19. Guo, Z.Y., Duan, J., Yang, F., Li, M., Hao, T.T., Wang, S., Wei, D.Y.: A test strip platform based on DNA functionalized gold nanoparticles for on-site detection of mercury (II) ions. Talanta **93**, 49–54 (2012)
20. Xie, W.Y., Huang, W.T., Zhang, J.R., Luo, H.Q., Li, N.B.: A triple-channel optical signal probe for Hg^{2+} detection based on acridine orange and aptamer-wrapped gold nanoparticles. J. Mater. Chem. **22**, 11479–11482 (2012)
21. Ma, Y.J., Jiang, L., Mei, Y.J., Song, R.B., Tian, D.B., Huang, H.: Colorimetric sensing strategy for mercury(II) and melamine utilizing cysteamine-modified gold nanoparticles. Analyst **138**, 5338–5343 (2013)
22. Tao, Y., Lin, Y.H., Huang, Z.Z., Ren, J.S., Qu, G.: Poly(acrylic acid)-templated silver nanoclusters as a platform for dual

fluorometric turn-on and colorimetric detection of mercury (II) ions. Talanta **88**, 290–294 (2012)
23. Yuan, X., Wen, S.H., Shen, M.W., Shi, X.Y.: Dendrimer-stabilized silver nanoparticles enable efficient colorimetric sensing of mercury ions in aqueous solution. Anal. Methods **5**, 5486–5492 (2013)
24. Xin, J.W., Zhang, F.Q., Gao, Y.X., Feng, Y.Y., Chen, S.G., Wu, A.G.: A rapid colorimetric detection method of trace Cr(VI) based on the redox etching of Ag_{core}–Au_{shell} nanoparticles at room temperature. Talanta **101**, 122–127 (2012)
25. Lou, T.T., Chen, L.X., Chen, Z.P., Wang, Y.Q., Chen, L., Li, H.: Colorimetric detection of trace copper ions based on catalytic leaching of silver-coated gold nanoparticles. Appl. Mater. Interf. **3**, 4215–4220 (2011)
26. Huang, L., Zhang, Z.: Label-free electrochemical DNA biosensor based on a glassy carbon electrode modified with gold nanoparticles, polythionine, and grapheme. Microchim. Acta **176**, 463–470 (2012)
27. Liu, F.K., Tsai, M.H., Hsuc, Y.C., Chub, T.C.: Analytical separation of Au/Ag core/shell nanoparticles by capillary electrophoresis. J. Chromatogr. A **1133**, 340–346 (2006)
28. Lin, C.Y., Yu, C.J., Lin, Y.H., Tseng, L.: Colorimetric sensing of silver(I) and mercury(II) ions based on an assembly of tween 20-stabilized gold nanoparticles. Anal. Chem. **82**, 6830–6837 (2010)